GEOLOGY | THE GEOLOGICAL SOCIETY OF AMERICA®

https://doi.org/10.1130/G45180.1

Manuscript received 21 May 2018
Revised manuscript received 2 October 2018
Manuscript accepted 8 October 2018

Published online 23 October 2018

Oceanic origin of continental mantle lithosphere

Andrea Servali* and Jun Korenaga
Department of Geology and Geophysics, Yale University, PO Box 208109, New Haven, Connecticut 06520-8109, USA

ABSTRACT

We present a global compilation of major element, as well as Re-Os isotope, data on mantle xenoliths from continental lithosphere to constrain the secular evolution of mantle depletion since the early Archean. Whereas a temporal dichotomy in the degree of mantle depletion has long been recognized in previous regional studies of mantle xenoliths, this global compilation reveals, for the first time, a smooth secular trend in mantle depletion, which is in remarkable agreement with what is expected from the secular cooling of the ambient mantle as inferred from the petrology of non-arc basalts. Depleted mantle now composing continental lithosphere is likely to have been originally formed beneath mid-ocean ridges or similar spreading environments, and a greater degree of depletion in the past can be seen as a corollary of the secular cooling of the mantle.

INTRODUCTION

A plethora of evidence from tomographic imaging and petrological observations on mantle xenoliths corroborates the existence of thermally and chemically distinct continental mantle lithosphere underlying most Archean and Proterozoic exposed landmasses (e.g., Carlson et al., 2005). Petrological analyses of cratonic mantle xenoliths from Archean and Proterozoic terranes indicate a mantle predominantly composed of highly depleted peridotites (e.g., Boyd, 1989; Pearson and Wittig, 2008). The degree of depletion is commonly described by Mg#, which is molar Mg / (Mg + Fe) × 100, and a higher Mg# results from a higher degree of melting. The average Mg# of cratonic xenoliths is ~92, reaching as high as 94 for some Archean samples, whereas typical fertile peridotites in the present asthenospheric mantle have a Mg# ~88–89. The Mg# of mantle xenoliths has long been known to exhibit a temporal dichotomy; samples collected from Archean cratons are characterized by higher levels of depletion compared to those from Proterozoic and Phanerozoic provinces (Boyd, 1989; Kelemen et al., 1998; Griffin et al., 2008).

The existence of highly depleted mantle has led to two popular hypotheses for the origin of continental mantle lithosphere: one involving oceanic ridges (e.g., Herzberg, 2004; Rollinson, 2010; Pearson and Wittig, 2014) and the other involving mantle plumes (e.g., Herzberg, 1999; Aulbach et al., 2011). Additional depletion in arc settings has also been suggested (e.g., Pearson and Wittig, 2008). Resolving the origin of continental lithosphere has been difficult because the occurrence of mantle xenoliths is spatially limited and the geological record of old continental crust is generally complex. In this study, we aim to test the oceanic ridge hypothesis on the basis of a global compilation of mantle xenolith data. One attractive feature of this hypothesis is that it makes a definitive prediction for the secular compositional trend of mantle depletion (Herzberg and Rudnick, 2012) against which xenolith data can be compared. Whereas a contrast in the degree of depletion between Archean and Proterozoic xenoliths has long been known, as noted above, a detailed picture of how mantle depletion has changed through time is yet to be established. To this end, we assemble major element composition (i.e., MgO and FeO), as well as Re-Os isotope data, for mantle xenoliths found on major cratons.

In what follows, we first provide essential traits of the cratons and xenoliths we consider in this study. Such information aids in interpretation of the wide range of ages and chemical compositions present in our global compilation. We then describe our strategy for data compilation to extract the temporal evolution of mantle depletion. Finally, we discuss a possible origin of continental mantle lithosphere via mid-ocean ridge processes, on the basis of a correlation between the emerged trend of mantle depletion and the secular cooling of the upper mantle.

MANTLE XENOLITHS

The chemical composition of continental mantle lithosphere is highly variable around the globe. Whereas Archean and younger cratons are generally underlain by highly depleted mantle and less-depleted mantle, respectively, each craton has been affected by its own tectonic history. Commonly, the degree of complexity observed in surface geology is coupled with an equivalent amount of deformation in the mantle (e.g., Carlson et al., 2005). As a result, the mantle lithosphere preserves changes in major and minor element compositions correlated to tectonic processes, such as metasomatism, that affect interpretation of data. To account for possible modifications of the original Mg# and Re-Os isotope system, it is important to focus on geological areas that have been thoroughly studied, with a statistically sufficient number of whole-rock analyses (Rudnick and Walker, 2009). Except for some Mesozoic and Paleozoic peridotite xenoliths retrieved in alkaline basalts from the China blocks, mantle xenoliths in our compilation were collected in kimberlite pipes that erupted between the Proterozoic and the Mesozoic (e.g., Irvine et al. 2003; Pearson et al., 2007; Wittig et al., 2010; Liu et al., 2012). Good age correlation is generally observed between model ages of mantle xenoliths and ages of crustal rocks, suggesting a coupling between crustal and mantle lithosphere (Rollinson, 2010); notable exceptions to this general trend are the Sino-Korean craton and the South China block. The data set includes samples from the Churchill province (Canada); Kaapvaal (southern Africa), Tanzania, North and South China, North Atlantic (Greenland), Slave (Canada), Siberian, and Karelian (Finland and Russia) cratons; and Wyoming province (USA and Canada) (sample locations, source references, and data are provided in the GSA Data Repository[1], along with a summary of

[1]GSA Data Repository item 2018397, supplementary information on surface geology of cratons, supplementary figures, and Table DR1(data and sources for all cratons), is available online at http://www.geosociety.org/datarepository/2018/ or on request from editing@geosociety.org.

*E-mail: andrea.servali@yale.edu

CITATION: Servali, A., and Korenaga, J., 2018, Oceanic origin of continental mantle lithosphere: Geology, v. 46, p. 1047–1050, https://doi.org/10.1130/G45180.1

notable surface geology characteristics for each of these cratons).

METHODS AND RESULTS

During the partial melting of the mantle, Fe and Re are partitioned into the melt phase more preferentially than Mg and Os, respectively. Such a contrast in element partitioning is central to quantifying the degree of melting and its timing, the former by Mg-Fe partitioning and the latter by Re-Os model ages. For Mg-Fe partitioning, we consider both olivine and whole-rock Mg#. Re-Os model ages rely on sulfides that are susceptible to secondary processes and thus are not expected to provide accurate ages; numerous pre-, syn-, and post-eruption chemical interactions between melt and residue commonly alter Re and Os concentrations, thereby perturbing estimates on the timing of mantle depletion (Pearson and Wittig, 2008; Liu et al., 2010). Such model ages, however, represent the only effective method to constrain the timing of mantle depletion (Rudnick and Walker, 2009). Fortunately, two different types of model ages, Re depletion (T_{RD}) and mantle (T_{MA}) model ages, have been devised (Walker et al., 1989), which allow discussion of the reliability of age estimates (Carlson et al., 2005; Pearson and Wittig, 2008).

The majority of the published Re-Os isotope data for mantle xenoliths are based on whole-rock analysis. Unlike sulfide analysis, whole-rock analysis does not allow probing of the possibility of secondary metasomatism, but model ages based on whole-rock analyses generally reflect the age of crystalline basement or later tectonic deformation (Griffin et al., 2004; Pearson and Wittig, 2014). We thus adopt whole-rock T_{RD} and T_{MA} model ages as the lower and upper limits on mantle depletion age, respectively. To ensure the uniform treatment of data, we recompute both T_{RD} and T_{MA} model ages for the entire data set using the estimate of the primordial $^{187}Re/^{188}Os$ and $^{187}Os/^{188}Os$ by Walker et al. (2002), though this recomputation does not change the overall secular trend. We adopt the carbonaceous chondrite standard as it likely represents the isotopic signature of Earth's primitive mantle (Korenaga, 2008b). Employing the carbonaceous chondrite standard systematically produces younger ages than using other reference values, with age differences as large as 500 m.y. for young samples (see the Data Repository). Most of the data compiled here have been corrected for Re contamination during host magma entrainment (Shirey and Walker, 1998; Pearson et al., 2004). Between T_{RD} and T_{MA}, T_{RD} is usually considered to be more robust because Os is less affected by metasomatism. We thus place more weight on T_{RD} model ages and discard any T_{MA} model ages differing by >1 b.y. from T_{RD}, as they likely suffer from secondary enrichment of Re. Further, we omit T_{MA} and T_{RD} ages with future values or older than the age of the Earth (i.e., 4.5 Ga).

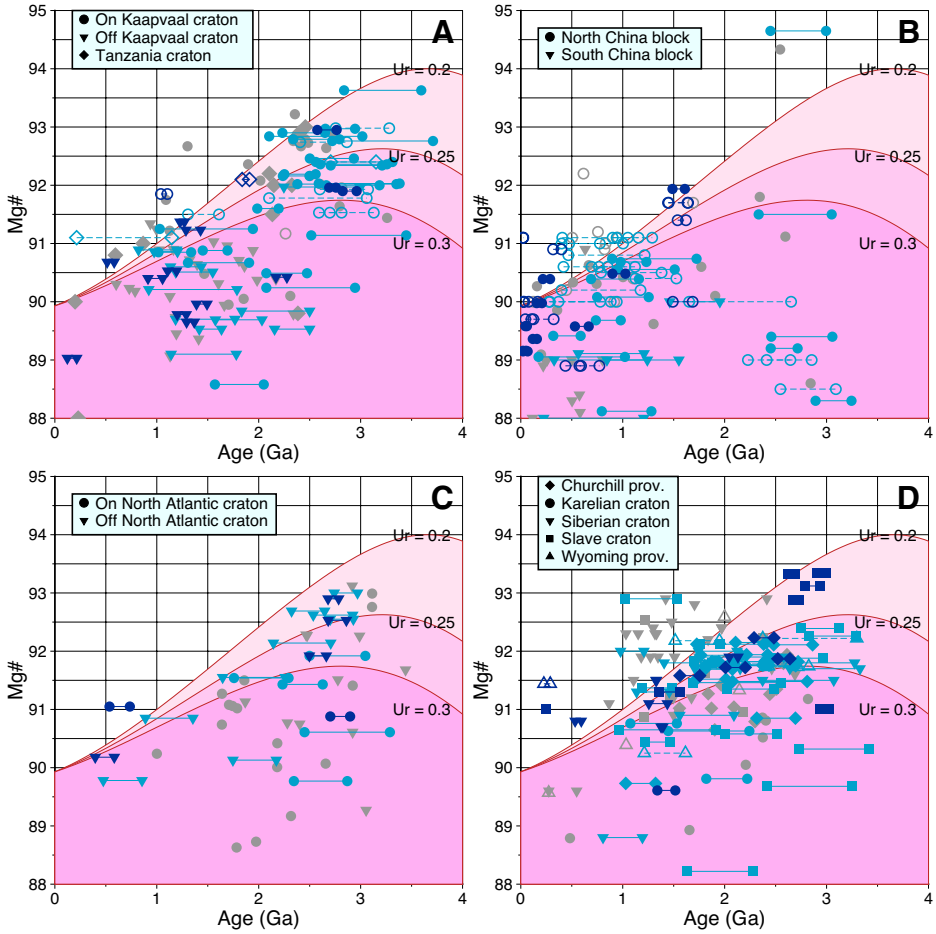

Figure 1. Covariation of whole-rock Mg# [molar Mg / (Mg + Fe) × 100] and model ages for mantle xenoliths from Kaapvaal and Tanzania cratons, Africa (A), China cratons (B), the North Atlantic craton (C), and other major cratons (see text for locations (D). (prov.—province) For the majority of data, both Re depletion (T_{RD}) and mantle (T_{MA}) model ages are shown (with T_{MA} being older). Solid symbols denote T_{RD} model ages corrected for eruption contamination, whereas open symbols denote those uncorrected. Dark blue symbols connected with line denote data with $T_{MA} - T_{RD} < 0.2$ b.y. Light blue symbols are used for data with $T_{MA} - T_{RD} < 1$ b.y. Symbols connected by dashed line are used for data uncorrected for eruption contamination. Gray symbols represent T_{RD} ages for data with T_{MA} >1 b.y. apart from T_{RD} or with only T_{RD} ages reported. Our coding of symbols is to place greater emphasis (bolder colors) on more reliable data. Shown in pink shading is range of Mg# corresponding to thermal evolution model of Korenaga (2017) for three different values of Urey ratio (Ur, the contribution of internal heat production to planetary-scale energy balance). Parameterization of Herzberg and Rudnick (2012) is used to convert mantle potential temperature to Mg# of mantle residue.

In Figure 1, the covariation of depletion age and whole-rock Mg# is shown for different groups of cratons. Figure 1A includes data collected on the Kaapvaal craton, its surrounding accreted Proterozoic terranes, and the Tanzania craton. Xenoliths from the Kaapvaal craton show depletion ages mostly between 2 and 3.5 Ga, those from the Proterozoic terranes between 0.5 and 2.5 Ga, and those from the Tanzania craton between the Paleozoic and the Archean. If we view these data collectively, a smooth trend in the age-Mg# covariation emerges, and it can be seen more clearly in olivine analysis (Fig. DR1A in the Data Repository). In line with previous studies, the eastern China data set (Fig. 1B) exhibits two distinct age populations; the majority of data plot between present and 1.5 Ga, whereas a small subset of ages ranges between 2.5 and 3.5 Ga. Whereas samples with older ages could be attributed to original mantle depletion, corresponding Mg# values are lower than observed for similarly old xenoliths from other cratons. The majority of T_{RD} ages for Phanerozoic and late Proterozoic samples likely have higher uncertainties due to inefficient extraction of Re at lower degrees of partial melting, and the ages of those samples could be older than shown in Figure 1B. Figure 1C shows data from the North Atlantic craton and its surrounding terranes. The age population is mostly between the Neoarchean and the Mesoarchean, corresponding to overlying crustal ages, yet some samples retain younger ages spanning through the Proterozoic. Whereas Paleoproterozoic and

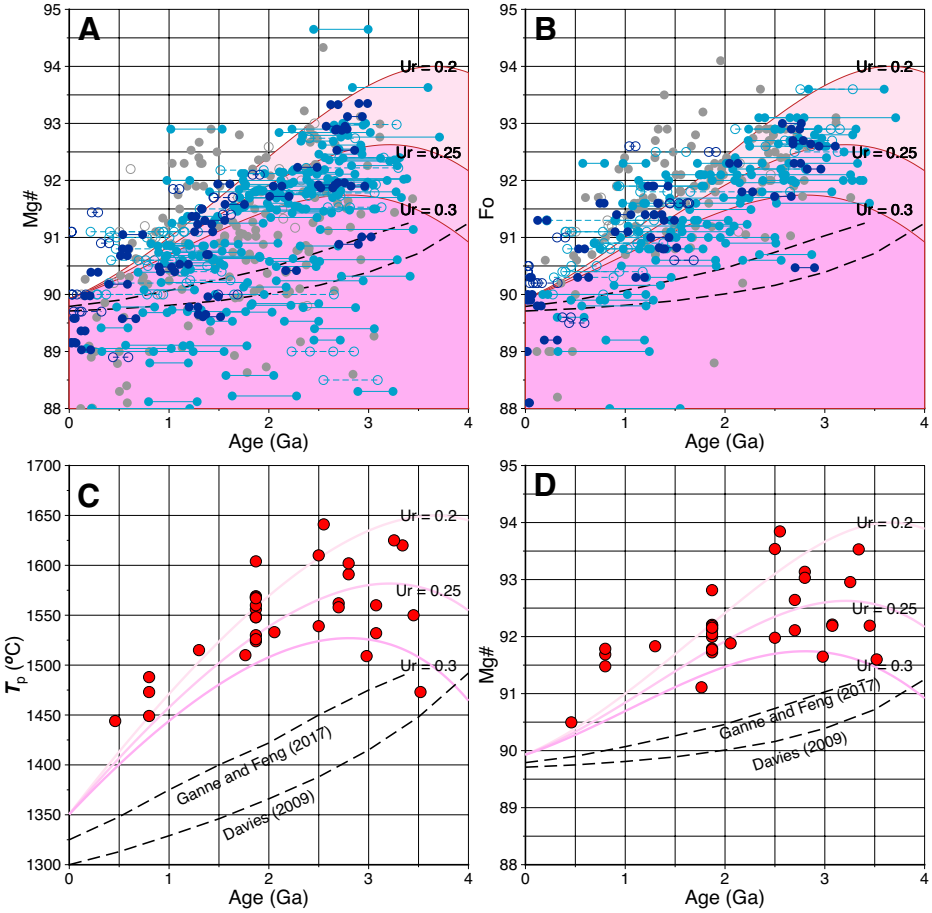

Figure 2. A: Covariation of whole-rock Mg# [molar Mg / (Mg + Fe) × 100] and model ages for global compilation of mantle xenolith data (symbols as in Figure 1). B: Same as A but with olivine forsterite (Fo) content. C: Evolution of mantle potential temperature (T_p) based on petrology of Precambrian igneous rocks (Herzberg et al., 2010). D: Mg# of mantle residue corresponding to igneous rocks shown in C (Herzberg and Rudnick, 2012). As in Figure 1, predictions based on thermal evolution model of Korenaga (2017) are shown in all panels (Ur—Urey ratio [the contribution of internal heat production to planetary-scale energy balance]). For comparison, predictions based on those of Davies (2009) and Ganne and Feng (2017) are also shown as dashed lines.

Mesoproterozoic ages could be associated with the amalgamation of other Archean terrains to the North Atlantic craton during the Proterozoic Nagssugtoqidian orogeny or rifting associated with the Kangâmiut dike swarm (both in western Greenland; Wittig et al., 2010), younger Precambrian ages do not have direct correlation to surface geology. We note that there is no clear age separation between xenoliths from the North Atlantic craton and those from its surroundings. The rest of the cratons we studied are shown collectively in Figure 1D. Despite the large variety, the majority of data cluster from the Proterozoic to the Archean, with Mg# ranging between 89 and 93.5.

Also shown in Figure 1 are the predictions for Mg# variations based on the thermal evolution of the mantle (Korenaga, 2008a, 2017). The model of Korenaga (2017) is an updated version of that of Korenaga (2008a), with the former incorporating a more likely thermal history of the core. Three different predictions are given to take into account the uncertainty of the thermal budget; the present-day Urey ratio, which measures the ratio of radiogenic heat production in the mantle over convective heat loss, is estimated to be ~0.2–0.3 (Korenaga, 2017).

When viewed collectively (Figs. 2A and 2B), whole-rock and olivine data exhibit a positive trend between Mg# and age. Whole-rock data show greater scatter than olivine data (Fig. 2B), with Mg# as low as 88 seen at all ages, but the positive trend is seen for the maximum Mg# values; Mg# values of Archean, Proterozoic, and Phanerozoic xenoliths do not generally exceed ~93.5, ~92, and ~91, respectively. A tighter trend can be seen for the olivine forsterite (Fo) content (Fig. 2B). This positive trend between Mg# (or Fo) and age has important implications for the origin of continental lithospheric mantle, as discussed next.

IMPLICATIONS FOR THE ORIGIN OF CONTINENTAL LITHOSPHERE

Mantle xenoliths represent important direct samples of continental lithospheric mantle, but their sampling relies largely on fortuitous kimberlite magmatism. As such, the geographical distribution of mantle xenoliths is sparse and sporadic, and these xenoliths by no means sample continental lithosphere uniformly. The formation of continental lithosphere and its subsequent growth may have been episodic and stochastic, and xenolith sampling could be too sparse to understand such lithospheric evolution on a regional basis. Our approach based on a global compilation is an attempt to set aside regional complexities in favor of gross characteristics of continental lithospheric mantle as a whole. Perhaps the most important result that emerged from our global compilation is that the positive correlation between the Fo contents of mantle xenoliths and their ages, spanning from the present to 3 Ga, are in remarkable agreement with the prediction from the thermal evolution model (Fig. 2B). Regional data do not exhibit this trend with comparable clarity (Fig. 1; Fig. DR1). Increasing Fo or Mg# with age can be understood to have resulted from a higher degree of melting of a hotter mantle in the past (Herzberg et al., 2010; Herzberg and Rudnick, 2012), and the covariation of xenolith mineralogy and ages (Fig. DR2) supports this interpretation; in general, we observe that the majority of lherzolite xenoliths are grouped in the Phanerozoic and late Proterozoic, and harzburgites are concentrated between the early Proterozoic and Archean.

Greater scatter seen in the whole-rock Mg# trend (Fig. 2A) than in the Fo trend (Fig. 2B) could result from several processes. For example, the presence of interstitial FeO at grain boundaries (Pearson and Wittig, 2014), secondary processes such as serpentinization, and the invasive nature of kimberlite (Schmidberger and Francis, 2001) could all change whole-rock Mg#. At any given time, Fo contents exhibit variability of ~1.5 Fo units, but this variability is part of the total variability expected from polybaric decompressional melting, in which whole-rock Mg# or olivine Fo content ranges from an initial fertile value (88–89) to the most depleted value, as indicated by shading associated with theoretical predictions shown in Figures 1 and 2 (Herzberg et al., 2010). For early Proterozoic and Archean samples, the age-Fo covariation plot does not show the relatively fertile part of this spectrum (i.e., Fo unit <90), suggesting that the less-depleted part was mechanically too weak to remain in the continental lithosphere. In decompressional melting beneath mid-ocean ridges, only the mantle that reaches shallow depths experiences a high degree of melting and can become mechanically strong due to surface cooling.

The thermal evolution model used here is based on the notion of more sluggish plate tectonics in the past (Korenaga, 2003), and this model predicts a particular cooling curve for the upper mantle, which is supported by the

petrology of Precambrian lavas (Herzberg et al., 2010; Fig. 2C). Herzberg and Rudnick (2012) estimated the secular evolution of Mg# of the residual mantle corresponding to those lavas (Fig. 2D), which is similar to the Fo trend seen in our compilation (Fig. 2B). This similarity is rather remarkable because these diagrams present two entirely independent kinds of geochemical data one from non-arc basalts and the other from cratonic mantle xenoliths. It would be most straightforward to interpret this coincidence as support for a mid-ocean ridge origin of continental lithospheric mantle. That is, depleted mantle now composing continental lithosphere was originally formed beneath mid-ocean ridges or similar spreading environments, and a greater degree of depletion in the past is a corollary of the secular cooling of the mantle. This simple theoretical framework for the origin of continental lithospheric mantle, which is built on the thermal evolution of Earth, may prove useful as a reference when investigating the formation history of lithospheric mantle beneath individual cratons. Such a framework also facilitates the theoretical analysis of the surface environment on early Earth, as the secular evolution of continental lithosphere plays a dominant role in global sea-level change (Korenaga et al., 2017).

ACKNOWLEDGMENTS

This material is based upon work supported by the NASA through the NASA Astrobiology Institute under Cooperative Agreement No. NNA15BB03A issued through the Science Mission Directorate. This study was motivated by a question raised by David Evans. The authors thank Claude Herzberg and Dante Canil for constructive reviews.

REFERENCES CITED

Aulbach, S., Stachel, T., Heaman, L.M., Creaser, R.A., and Shirey, S.B., 2011, Formation of cratonic subcontinental lithospheric mantle and complementary komatiite from hybrid plume sources: Contributions to Mineralogy and Petrology, v. 161, p. 947–960, https://doi.org/10.1007/s00410-010-0573-4.

Boyd, F.R., 1989, Compositional distinction between oceanic and cratonic lithosphere: Earth and Planetary Science Letters, v. 96, p. 15–26, https://doi.org/10.1016/0012-821X(89)90120-9.

Carlson, R.W., Pearson, D.G., and James, D.E., 2005, Physical, chemical, and chronological characteristics of continental mantle: Reviews of Geophysics, v. 43, RG1001, https://doi.org/10.1029/2004RG000156.

Davies, G.F., 2009, Effect of plate bending on the Urey ratio and the thermal evolution of the mantle: Earth and Planetary Science Letters, v. 287, p. 513–518, https://doi.org/10.1016/j.epsl.2009.08.038.

Ganne, J., and Feng, X., 2017, Primary magmas and mantle temperatures through time: Geochemistry Geophysics Geosystems, v. 18, p. 872–888, https://doi.org/10.1002/2016GC006787.

Griffin, W.L., Graham, S., O'Reilly, S.Y., and Pearson, N.J., 2004, Lithosphere evolution beneath the Kaapvaal Craton: Re-Os systematics of sulfides in mantle-derived peridotites: Chemical Geology, v. 208, p. 89–118, https://doi.org/10.1016/j.chemgeo.2004.04.007.

Griffin, W.L., O'Reilly, S.Y., Afonso, J.C., and Begg, G.C., 2008, The composition and evolution of lithospheric mantle: A re-evaluation and its tectonic implications: Journal of Petrology, v. 50, p. 1185–1204, https://doi.org/10.1093/petrology/egn033.

Herzberg, C., 1999, Phase equilibrium constraints on the formation of cratonic mantle, *in* Fei, Y., et al., eds., Mantle Petrology: Field Observations and High Pressure Experimentation: A Tribute to Francis R. (Joe) Boyd: Geochemical Society Special Publication 6, p. 241–257.

Herzberg, C., 2004, Geodynamic information in peridotite petrology: Journal of Petrology, v. 45, p. 2507–2530, https://doi.org/10.1093/petrology/egh039.

Herzberg, C., and Rudnick, R., 2012, Formation of cratonic lithosphere: An integrated thermal and petrological model: Lithos, v. 149, p. 4–15, https://doi.org/10.1016/j.lithos.2012.01.010.

Herzberg, C., Condie, K., and Korenaga, J., 2010, Thermal history of the Earth and its petrological expression: Earth and Planetary Science Letters, v. 292, p. 79–88, https://doi.org/10.1016/j.epsl.2010.01.022.

Irvine, G.J., Pearson, D.G., Kjarsgaard, B.A., Carlson, R.W., Kopylova, M.G., and Dreibus, G., 2003, A Re-Os isotope and PGE study of kimberlite-derived peridotite xenoliths from Somerset Island and a comparison to the Slave and Kaapvaal cratons: Lithos, v. 71, p. 461–488, https://doi.org/10.1016/S0024-4937(03)00126-9.

Kelemen, P.B., Hart, S.R., and Bernstein, S., 1998, Silica enrichment in the continental upper mantle via melt/rock reaction: Earth and Planetary Science Letters, v. 164, p. 387–406, https://doi.org/10.1016/S0012-821X(98)00233-7.

Korenaga, J., 2003, Energetics of mantle convection and the fate of fossil heat: Geophysical Research Letters, v. 30, 1437, https://doi.org/10.1029/2003GL016982.

Korenaga, J., 2008a, Urey ratio and the structure and evolution of Earth's mantle: Reviews of Geophysics, v. 46, RG2007, https://doi.org/10.1029/2007RG000241.

Korenaga, J., 2008b, Plate tectonics, flood basalts and the evolution of Earth's oceans: Terra Nova, v. 20, p. 419–439, https://doi.org/10.1111/j.1365-3121.2008.00843.x.

Korenaga, J., 2017, Pitfalls in modeling mantle convection with internal heat production: Journal of Geophysical Research: Solid Earth, v. 122, p. 4064–4085, https://doi.org/10.1002/2016JB013850.

Korenaga, J., Planavsky, N.J., and Evans, D.A.D., 2017, Global water cycle and the coevolution of the Earth's interior and surface environment: Philosophical Transactions of the Royal Society A, v. 375, 20150393, https://doi.org/10.1098/rsta.2015.0393.

Liu, C.-Z., Liu, Z.-C., Wu, F.-Y., and Chu, Z.-Y., 2012, Mesozoic accretion of juvenile sub-continental lithospheric mantle beneath South China and its implications: Geochemical and Re-Os isotopic results from Ningyuan mantle xenoliths: Chemical Geology, v. 291, p. 186–198, https://doi.org/10.1016/j.chemgeo.2011.10.006.

Liu, J., Rudnick, R.L., Walker, R.J., Gao, S., Wu, F., and Piccoli, P.M., 2010, Processes controlling highly siderophile element fractionations in xenolithic peridotites and their influence on Os isotopes: Earth and Planetary Science Letters, v. 297, p. 287–297, https://doi.org/10.1016/j.epsl.2010.06.030.

Pearson, D.G., and Wittig, N., 2008, Formation of Archaean continental lithosphere and its diamonds: The root of the problem: Journal of the Geological Society, v. 165, p. 895–914, https://doi.org/10.1144/0016-76492008-003.

Pearson, D.G., and Wittig, N., 2014, The formation and evolution of cratonic mantle lithosphere—Evidence from mantle xenoliths, *in* Holland, H.D., and Turekian, K.K., eds., Treatise on Geochemistry (second edition): Amsterdam, Elsevier, p. 255–292, https://doi.org/10.1016/B978-0-08-095975-7.00205-9.

Pearson, D.G., Irvine, G.J., Ionov, D.A., Boyd, F.R., and Dreibus, G.E., 2004, Re-Os isotope systematics and platinum group element fractionation during mantle melt extraction: A study of massif and xenolith peridotite suites: Chemical Geology, v. 208, p. 29–59, https://doi.org/10.1016/j.chemgeo.2004.04.005.

Pearson, D.G., Parman, S.W., and Nowell, G.M., 2007, A link between large mantle melting events and continent growth seen in osmium isotopes: Nature, v. 449, p. 202–205, https://doi.org/10.1038/nature06122.

Rollinson, H., 2010, Coupled evolution of Archean continental crust and subcontinental lithospheric mantle: Geology, v. 38, p. 1083–1086, https://doi.org/10.1130/G31159.1.

Rudnick, R.L., and Walker, R.J., 2009, Interpreting ages from Re-Os isotopes in peridotites: Lithos, v. 112, p. 1083–1095, https://doi.org/10.1016/j.lithos.2009.04.042.

Schmidberger, S.S., and Francis, D., 2001, Constraints on the trace element composition of the Archean mantle root beneath Somerset Island, Arctic Canada: Journal of Petrology, v. 42, p. 1095–1117, https://doi.org/10.1093/petrology/42.6.1095.

Shirey, S.B., and Walker, R.J., 1998, The Re-Os isotope system in cosmochemistry and high-temperature geochemistry: Annual Review of Earth and Planetary Sciences, v. 26, p. 423–500, https://doi.org/10.1146/annurev.earth.26.1.423.

Walker, R.J., Carlson, R.W., Shirey, S.B., and Boyd, F.R., 1989, Os, Sr, Nd, and Pb isotope systematics of southern African peridotite xenoliths: Implications for the chemical evolution of subcontinental mantle: Geochimica et Cosmochimica Acta, v. 53, p. 1583–1595, https://doi.org/10.1016/0016-7037(89)90240-8.

Walker, R.J., Horan, M.F., Morgan, J.W., Becker, H., Grossman, J.N., and Rubin, A.E., 2002, Comparative ^{187}Re-^{187}Os systematics of chondrites: Implications regarding early solar system processes: Geochimica et Cosmochimica Acta, v. 66, p. 4187–4201, https://doi.org/10.1016/S0016-7037(02)01003-7.

Wittig, N., Webb, M., Pearson, D.G., Dale, C.W., Ottley, C.J., Hutchison, M., Jensen, S.M., and Luguet, A., 2010, Formation of the North Atlantic Craton: Timing and mechanisms constrained from Re-Os isotope and PGE data of peridotite xenoliths from S.W. Greenland: Chemical Geology, v. 276, p. 166–187, https://doi.org/10.1016/j.chemgeo.2010.06.002.

Printed in USA